www.czasopisma.pan.pl PAN POLSKA AKADEMIA NAUK www.journals.pan.pl

Arch. Metall. Mater. **63** (2018), 2, 845-851

DOI: 10.24425/122413

S. LESZ*#, M. KREMZER*, K. GOŁOMBEK*, R. NOWOSIELSKI*

INFLUENCE OF MILLING TIME ON AMORPHIZATION OF Mg-Zn-Ca POWDERS SYNTHESIZED BY MECHANICAL ALLOYING TECHNIQUE

$Mg_{60}Zn_{35}Ca_5$ amorphous powder alloys were synthesized by mechanical alloying (MA) technique. The results of the influence of high-energy ball-milling time on amorphization of the $Mg_{60}Zn_{35}Ca_5$ elemental blend (intended for biomedical application) were presented in the study. The amorphization process was investigated by X-ray diffraction (XRD), scanning electron microscopy (SEM), transmission electron microscopy (TEM). Initial elemental powders were mechanically alloyed in a Spex 8000 high-energy ball mill at different milling times (from 3 to 24 h). Observation of the powder morphology after various stages of milling leads to the conclusion that with the increase of the milling time the size of the powder particles as well as the degree of aggregation change. The partially amorphous powders were obtained in the $Mg_{60}Zn_{35}Ca_5$ alloy after milling for 13-18h. The results indicate that this technique is a powerful process for preparing $Mg_{60}Zn_{35}Ca_5$ alloys with amorphous and nanocrystalline structure.

Keywords: Mg-based powders, Transmission electron microscopy, Scanning electron microscopy, Mechanicall alloying

1. Introduction

Magnesium-based materials were first introduced as orthopedic biomaterials in the first half of the century [1]. Mg-based alloys are regarded as highly promising engineered materials for expanding the possible applications of amorphous materials due to their light-weight and good mechanical properties. Magnesium with a density of 1.74 g/cm^3 has 4.5 times lower density than stainless steel, widely used in orthopaedic implantology [2]. Magnesium and magnesium based alloys have similar mechanical properties to natural bone [3,4]. The major drawback of magnesium in many engineering applications its corrosion resistance, especially in electrolytic environments, becomes an intriguing property for biomaterial applications, just like zirconium or titanium oxides [5-8]. The magnesium-based implant in the vivo corrosion involves the formation of a soluble, nontoxic oxide that is harmlessly excreted in the urine [9,10]. It is projected that magnesium and its alloys be applied as lightweight, degradable, load bearing orthopedic implants.

The production process is usually optimized for specific materials. The interrelationships among structure, properties, and performance of materials, and their modification by synthesis and processing, constitute the central theme of materials science and engineering [11-16]. Amorphization of alloys is thought to cause a significant increase in mechanical strength and corrosion resistance; consequently, a number of studies on the amorphization of Mg-based alloys have been carried out. In the last years, solid state amorphization has gained considerable importance as an alternate route to rapid solidification processing for the synthesis of amorphous phases [17,18]. A number of casting techniques are available to produce an amorphous metallic alloys. It has been reported that amorphous materials containing Mg as the main constituent element have been produced by casting method in various systems such as Mg-Cu-Y, Mg-Cu-Y-Al [19-22]. However, it has been difficult to prepare an amorphous Mg-based alloys of a large size. The maximum size of samples produced by rapid quenching techniques is only of the order of few millimetres for as-cast Mg-based systems [20,22]. To overcome the size and shape limitations of amorphous metallic alloys, there have been some attempts carried out to produce bulk amorphous alloys by powder metallurgy processing [23,24]. Among the various techniques of solid state amorphization, mechanical alloying (MA) has attracted wide spread attention due to its simplicity [25-28]. MA is a solid-state powder processing technique involving repeated welding, fracturing, and rewelding of powder particles in a high-energy ball mill. MA has now been shown to be capable of synthesizing a variety of non-equilibrium alloy phases starting from blended elemental or prealloyed powders. The non-equilibrium phases synthesized include supersaturated solid solutions, metastable crystalline phases, nanostructures, and amorphous alloys [18]. Mechanically alloyed powders are suitable for further processing; e.g. consolidation of bulk amorphous alloys by spark-plasma sintering [29,30]. The formation of an amorphous phases by MA of powder blends has been

* SILESIAN UNIVERSITY OF TECHNOLOGY, FACULTY OF MECHANICAL ENGINEERING, INSTITUTE OF ENGINEERING MATERIALS AND BIOMATERIALS, 18A KONARSKIEGO STR., 44-100 GLIWICE, POLAND

Corresponding author: sabina.lesz@polsl.pl

investigated in a variety of alloy systems during recent years [18,24,25,27,30-34]. However, very few reports exist on the effect of milling parameters on the amorphization.

This paper focuses on the influence of high-energy ball-milling time on the the evolution of amorphization of an elemental blend of composition $Mg_{60}Zn_{35}Ca_5$ system. The amorphous powder alloys were synthesized by MA.

2. Material and methods

2.1. Material

The elemental blends of compositions, used in the present study, have been obtained by thoroughly mixing high purity Mg (99.8 wt. %, −20 +100 mesh), Zn (99.9 wt. %, −100 mesh) and Ca (99.5 wt. %, −16 mesh) powders made by Alfa Aesar. Elemental powders of Mg, Zn and Ca were precisely measured to yield desired composition of $Mg_{60}Zn_{35}Ca_5$ (60 at.% Mg-35 at.% Zn-5 at.% Ca) alloy. SPEX 8000 high energy shaker ball mill was used for MA at room temperature. The milling was performed in an Ar atmosphere, minimizing the oxygen contamination. Milling was carried out with a ball to powder weight ratio of 10:1 in a stainless steel vial using 10 mm stainless steel balls. The MA process was carried out using selected time durations from 3 to 24 h. Each MA process was performed with 0.5 h interruptions. The powders and the milling balls were loaded into stainless steel vial under argon atmosphere and all the powders handling was performed in a glove box.

2.2. Experimental procedure

The milled samples were examined by X-ray diffraction (XRD), scanning electron microscopy (SEM), transmission electron microscopy (TEM), and differential scanning calorimetry (DSC). X-ray diffraction (XRD) using a X-Pert PRO MP diffractometer (PANalytical) with Co-K_α radiation of 1.7888 Å was used for analysis of the phase formation in the milled powder samples. The result of the analysis consists of an identified phase list with experimentally observed X-ray patterns and known diffraction patterns from various sources. The sources and the notation describing the quality of data are maintained by the ICDD (International Centre for Diffraction Data) [35]. The peaks were compared to probable crystalline species using the software X'Pert Highscore Plus 3.0e correlated with PAN-ICSD data base (PANalytical).

The particle morphology of the mechanically alloyed powder samples was observed by a SUPRA 35 scanning electron microscope (SEM) with a voltage of 20 kV (Carl Zeiss). The particles sizes distribution of the mechanically alloyed powder samples was determined in the granulometric analysis using a Laser Particle Size Analyzer (Fritsch Analysette 22-Nanotec), with an analysis field of 0,010-1000 µm. The most robust measures for discriminating between samples have been found to be the modal particle size, the median size (D_{50} value) [36].

Qualitatively and quantitative elemental analysis was performed using an EDAX energy-dispersive X-ray spectroscope (EDS), coupled with the SEM.

Transmission electron microscopy (TEM) observation was carried out in a (HRTEM) S/TEM TITAN 80-300 (FEI) microscope with a super twin lens operated at 300 kV. High-resolution electron microscope (HRTEM) images, selected area diffraction pattern (SADP) and nanobeam electron diffraction (NBED) patterns were collected. Samples for the transmission electron microscopy (TEM) study was prepared by powder dispersing in ethanol and deposition of obtained suspensions onto lacy carbon-coated copper grids.

The chemical composition was determined in the same apparatus using energy dispersive spectroscopy (EDS).

3. Results and discussion

The X-ray diffraction patterns of the $Mg_{60}Zn_{35}Ca_5$ powders after milling times ranging from 3 to 24 h are in Fig. 1. In the XRD

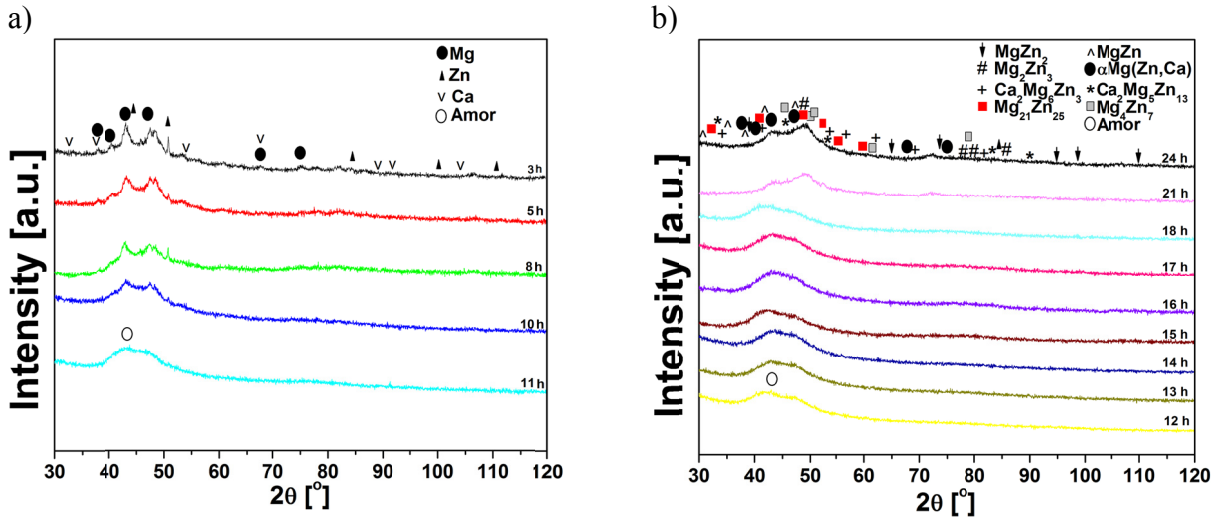

Fig. 1. Evolution of the X-ray diffraction pattern for the $Mg_{60}Zn_{35}Ca_5$ alloy milled for the time: a) from 3 up to 11 h, b) from 12 up to 24

patterns of the starting samples the Bragg reflections characteristic for the elemental Mg, Zn, Ca powders are noticed. After milling for 5, 8 and 10 h, the intensity of the crystalline Mg, Zn and Ca peaks decreased and a broad peak corresponding to the amorphous phase appeared. For the investigated alloy the amorphization occurs after 11 h of mechanical alloying. In their XRD patterns a broad diffraction peak is noticed, revealing the absence of the long range atomic order. No noticeable change in the phase composition was observed even after mechanical alloying for 18 h.

The XRD results were confirmed by a transmission electron microscopy (TEM) study on these powders (Fig. 2).

The high-resolution transmission electron micrograph (HRTEM) and the corresponding electron diffraction patterns of the $Mg_{60}Zn_{35}Ca_5$ powder alloy after milling for 13 h are given in Fig. 2a and Fig 2b, c, respectively. A selected area diffraction pattern (SADP) taken from one region shows a diffuse halo ring indicating the formation of the amorphous phase (Fig. 2b). Nano-beam electron diffraction (NBED) patterns from the other region shows the precipitate of nanocrystalline $MgZn_2$ phase (Fig. 2c) in the amorphous matrix. EDS microanalysis (Fig. 2d) indicate that the $Mg_{60}Zn_{35}Ca_5$ powder are composed of the alloyed elements Mg, Zn, and Ca. Presence of C and Cu is connected with carbon-coated copper TEM grids were used as substrate.

Further increase of milling time, from 21 up to 24 h, is leading to a mechanically induced crystallisation (Fig. 1b). It can be noticed that mechanically induced crystallisation leads to the formation of a certain amounts of crystalline a-Mg(Zn,Ca), MgZn, $MgZn_2$, Mg_2Zn_3, Mg_4Zn_7, $Mg_{21}Zn_{25}$, $Ca_5Mg_6Zn_3$, $Ca_2Mg_5Zn_{13}$ phases for the $Mg_{60}Zn_{35}Ca_5$ alloy. Similar results were also previously reported for mechanically induced crystallisation of $Mg_{60}Zn_{40-x}Ca_x$ (x = 0-20) powders of the 6 h of milling time [37].

An example of the particle size distribution for the $Mg_{60}Zn_{35}Ca_5$ alloy milled from 3 up to 24 h is presented in Fig. 3a-c. The particle size decreased gradually during the mill-

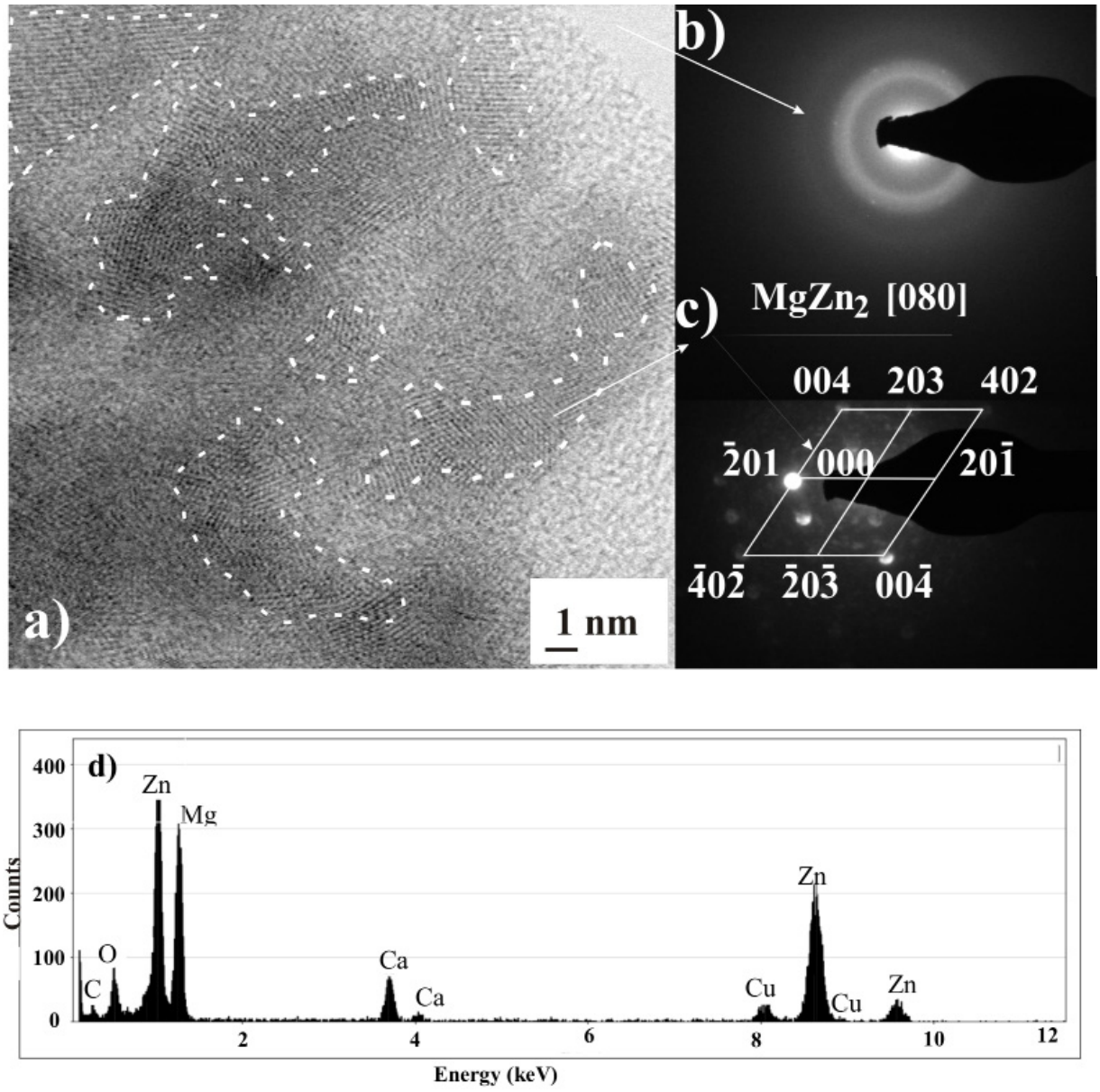

Fig. 2. Structure of the $Mg_{60}Zn_{35}Ca_5$ powders prepared by MA method after milling time 13 h; a) HRTEM image; b) electron diffraction from selected area marked with an arrow on Fig. a, confirm of an amorphous and c) nanocrystaline $MgZn_2$ phase; d) EDS spectrum

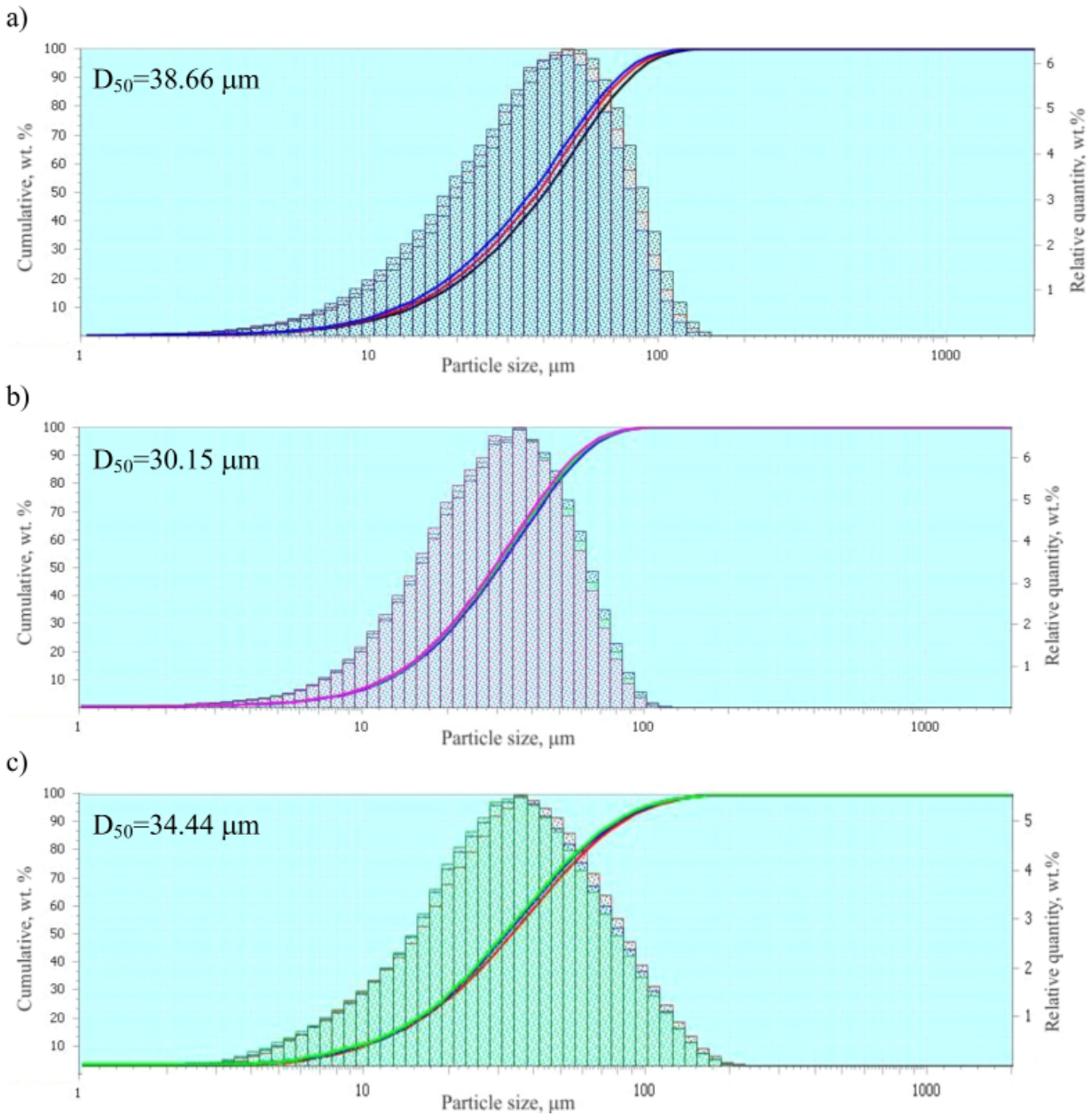

Fig. 3. Particle size distribution for the $Mg_{60}Zn_{35}Ca_5$ alloy milled from 3-24h: a) 3h, b) 13h, c) 24 h. For comparison reasons, the mean particle size (D_{50}) is given

ing times ranging from 11-13 h and 17-21h. There was decrease in particle size from 42.05 µm to 30.15 µm and from 30.11 µm to 24.17 µm after the milling times ranging from 11-13 h and 17-21h, respectively. Changes in the particle size and shape of the base powders are caused due to collisions with milling balls or with the milling container walls. All particles size distribution reveal a Gaussian like profile, which is given by the achievement of a balance between cold welding and fracturing phenomena induced by milling. This Gaussian distribution is favourable for the future compaction processes of the powders. The median particle diameter D_{50}, of the $Mg_{60}Zn_{35}Ca_5$ powder after milling for 13 h is 38.15 mm (Fig. 3b). In Fig. 4 is shown the evolution of the D_{50} parameter as a function of milling time. One can notice that the bimodal particle size distribution was kept during the milling times ranging from 13 to 18 h (example in Fig. 3b).

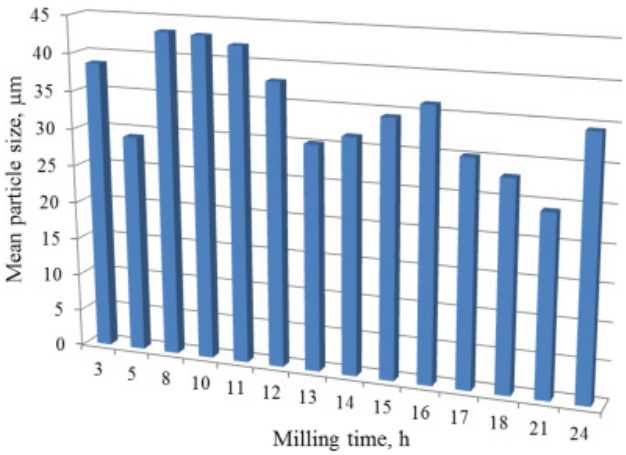

Fig. 4. Evolution of the D_{50} parameter versus milling time as derived from particle sizes distribution of the $Mg_{60}Zn_{35}Ca_5$ powder

The discrepancy between the two particle sizes is much less pronounced after milling for 13-18 h, than for milled powders in a shorter and longer time. The particle size being more homogeneous. This particle size distribution is very advantageous to be further processed because ensure density homogeneity and reduction of porosity.

The particles morphology evolution of ball-milled $Mg_{60}Zn_{35}Ca_5$ powders is shown in Fig. 5 a-i. The SEM investigation

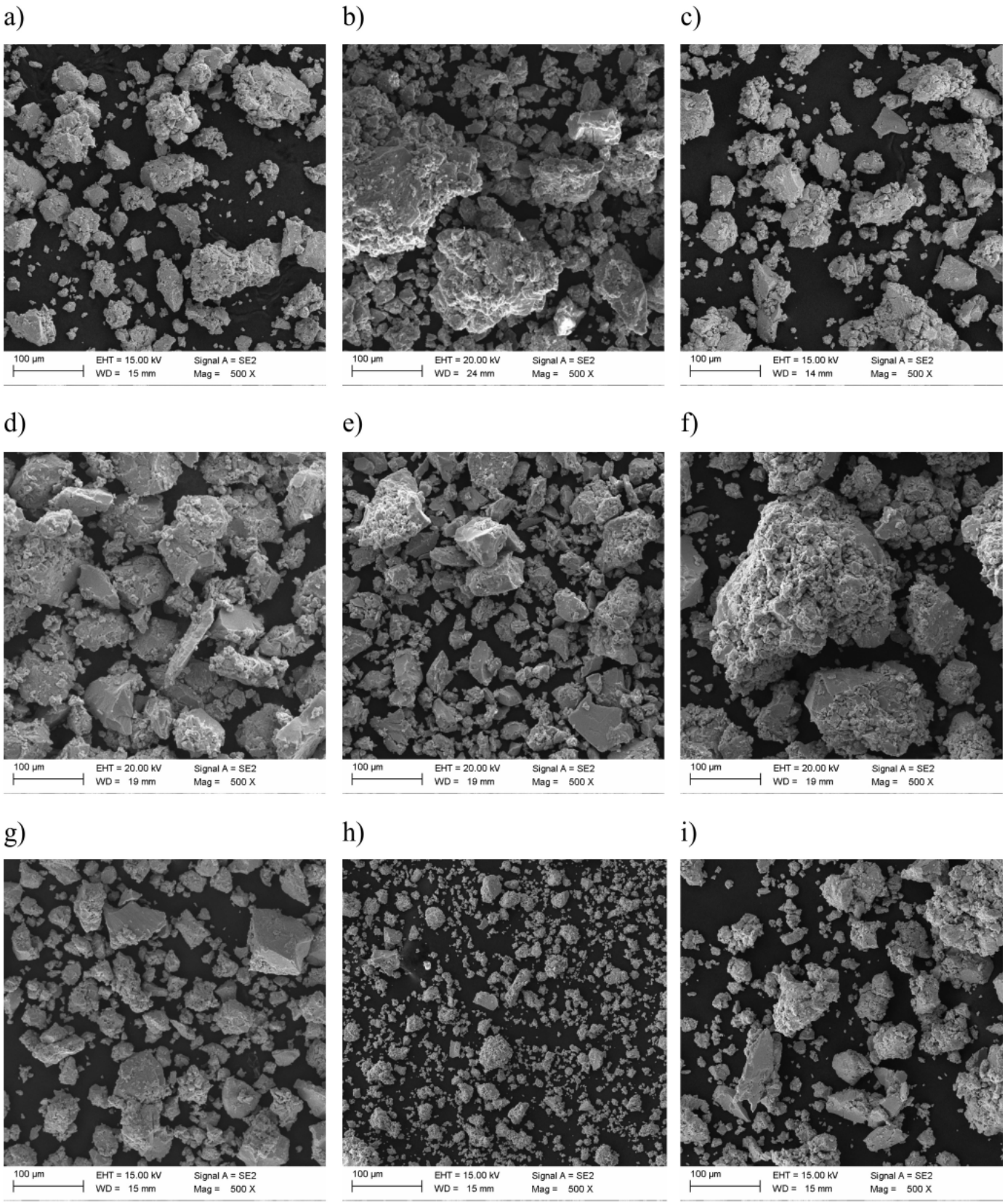

Fig. 5. The morphology of the $Mg_{60}Zn_{35}Ca_5$ particles after different times of milling (3-24h): a) 3h, b) 5h, c) 8h, d) 11 h, e) 13h, f) 15 h, g) 18 h, h) 21 h, i) 24 h, SEM

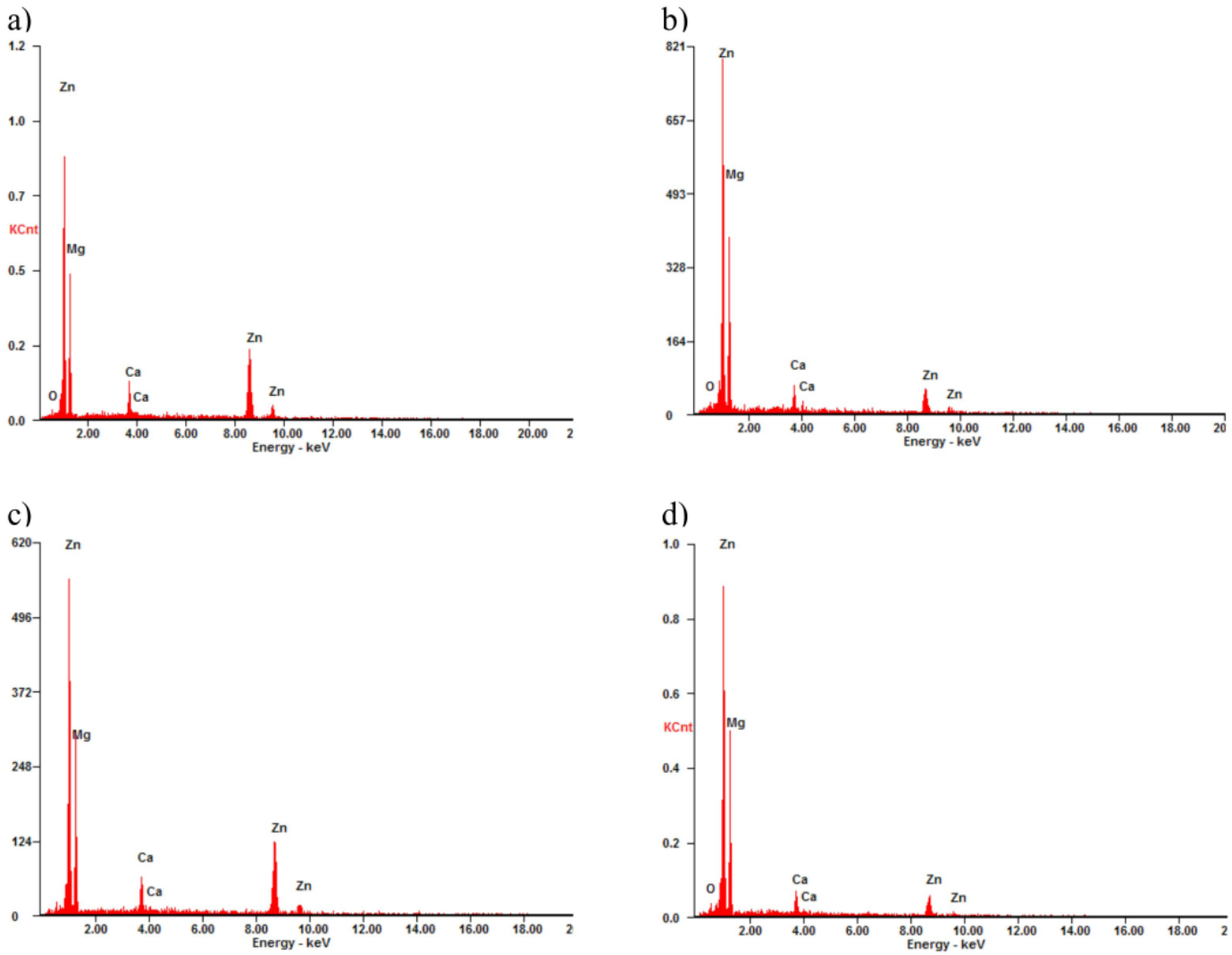

Fig. 6. The EDS spectrum of 5 (a), 8 (b), 13 h (c) and 24 h (d) milling time samples of the $Mg_{60}Zn_{35}Ca_5$ alloy

showed that powder is formed by particles with polyhedral shape. The SEM images reveal that the large particles are formed by smaller particles that are agglomerated and cold welded during milling [38]. For the $Mg_{60}Zn_{35}Ca_5$ powder after milling for 13 and 15 h, the particle size distribution shows the presence of certain amount of sub-micrometric particles. The presence of such particles was evidenced by SEM analysis. The presence of very fine particles on the surface of larger particles can be observed in Fig. 5 e, f.

The EDS spectrum of the 5, 8, 13 and 24 h milled samples shown in Fig. 6 a-d, reveals both constituent and oxygen elements. The oxygen contamination is expected and can be stemmed from powder handling. The oxygen atoms can be located on the surface of the powders due to their large surface areas.

The milling time required for amorphization in the $Mg_{60}Zn_{35}Ca_5$ alloy is 13 h. Similar observations regarding the glass-forming ability of the $Mg_{60}Zn_{35}Ca_5$ alloy were made by Datta et al. [39].

4. Conclusions

In conclusions, it was suggested that $Mg_{60}Zn_{35}Ca_5$ partially amorphous powder have been successfully generated by a non-equilibrium processing technique such as mechanical alloying (MA).

The results indicate that with the increase of the milling time the size of the powder particles as well as the degree of aggregation change. The partially amorphous powders were obtained in the $Mg_{60}Zn_{35}Ca_5$ alloy after milling for 13-18h. Synthesized $Mg_{60}Zn_{35}Ca_5$ powder are promising for future applications as new materials for orthopedic implants.

Acknowledgements

The work was supported by National Science Centre under research Project No.: 2013/09/B/ST8/02129.

REFERENCES

[1] A. Lambotte, Bull. Me´m Soc. Nat. Chir. **28**, 1325-1334 (1932).
[2] P.E. DeGarmo, Materials and processes in manufacturing, 5th ed. Collin Macmillan New York (1979).
[3] M. Razavi, M.H. Fathi, M. Meratian et al., Mater. Sci. Eng. A **527**, 26, 6938-6944 (2010).
[4] A. Feng, Y. Han, J. All. Comp. **504**, 585-593 (2010).
[5] A. Ziębowicz, B. Bączkowski, Numerical analysis of the implant – abutment system, in E. Piętka, J. Kawa (Eds.), Information Technologies in Biomedicine, LNBI 7339, 341-350, Springer-Verlag Berlin Heidelberg (2012).
[6] F. Živić, N. Grujović, G. Manivasagam, C. Richard , J. Landoulsi, V. Petrović, Tribol. Industry **36**, 1, 67-73 (2014).
[7] W. Kajzer, A. Kajzer, M. Grygiel-Pradelok, A. Ziębowicz, B. Ziębowicz, Adv. Intell. Syst. **2**, 385-398 (2016).
[8] D. Nakonieczny, A. Ziębowicz, Z. Paszenda, C. Krawczyk, Biocybern Biomed Eng. **37**, 1, 229-245 (2017)**.**
[9] C. Miura, Y. Shimizu, Y. Imai, et al., Biomed. Mater. **11**, 025001 (2016).
[10] M.P. Staiger, A. M. Pietak, J. Huadmai, G. Dias, Biomaterials **27**, 1728-1734 (2006).
[11] M.A. Meyers, K. K. Chawla: Mechanical Behavior of Materials, Cambridge University Press, The Edinburgh Building, Cambridge, 1-67 (2008).
[12] A. Drygała, L.A. Dobrzański, M. Szindler, M.M. Szindler, M.Prokopiuk vel Prokopowicz, E. Jonda, Int. J. Hydrogen. Energ. **41**, 18, 7563-7567 (2016).
[13] D. Szewieczek, S. Lesz, J. Mater. Process. Tech. **157**, 771-775 (2004).
[14] K. Drabczyk, G. Kulesza-Matlak, A, Drygała, M, Szindler, M. Lipiński, Sol. Energ. **126**, 14-21(2016).
[15] S. Lesz, Mater. Character. **124**, 97-106 (2017).
[16] A. Grajcar, A. Plachcinska, S. Topolska, M. Kciuk, Mater. Tehnol. **49**, 6, 889-894 (2015).
[17] W.L. Johnson, Prog. Mater. Sci. **30**, 81-134 (1986).
[18] C. Suryanarayana, Prog. Mater Sci. **46**, 1-184 (2001).
[19] A. Inoue, A. Kato, T. Zhang, S. G. Kim, T. Masumoto, JIM **32**, 7, 609-616 (1991).
[20] R. Babilas, R. Nowosielski, M. et al., Mater. Character. **102**, 156-164 (2015).
[21] N.H. Pryds, M. Eldrup, M. Ohuma et al., JIM **41**,11, 1435-1442 (2000).
[22] N.H. Pryds, Mater. Sci. Eng. A **375-377** 186-193 (2004).
[23] H.M. Lin, Y.W. Lin, P.Y. Lee, J. Mater. Sci. **43**, 3118-3123 (2008).
[24] H.V. Nguyen, J.S. Kim, Y.S. Kwon, J.C. Kim, J. Mater. Sci. **44**, 2700-2704 (2009).
[25] R. Amini, M.J. Hadianfard, E. Salahinejad, M. Marasi, T. Sritharan, J. Mater. Sci. **44**, 136-148 (2009).
[26] A.W. Weeber, H. Bakker, Physica B: Condensed Matter. **153**, 1-3, 93-135 (1988).
[27] P.Y. Lee, C.C. Koch, Appl. Phys. Lett. **50**, 1578-1580 (1987).
[28] T.S. Kim, J.K. Lee, H.J. Kim, J.C. Bae, Mater. Sci. Eng. A **402**, 228-233 (2005).
[29] Y.S. Lin, C.F. Hsu, J.Y. Chen, Y.M. Cheng, P.Y. Lee, Metals **6**, 11, 289, DOI:10.3390/met6110289 (2016).
[30] B.S. Murty, S. Ranganathan, M. M. Rao, Mater. Sci. Eng. A **149**, 231-240 (1992).
[31] R.B. Schwarz, C.C. Koch, Appl. Phys. Lett. **49**, 3, 146-148 (1986).
[32] G. Dercz, I. Matuła, M. Zubko, J. Dercz, Powder Diffr., DOI: 10.1017/S0885715617000045 (2017).
[33] R. Nowosielski, J.J. Wysłocki, I. Wnuk et al., J. Mater. Proc. Tech. **175**, 1-3, 324-329 (2006).
[34] Nowosielski; P. Gramatyka, P. Sakiewicz, R. Babilas, J. Magn. Magn. Mater. **387**, 179-185 (2015).
[35] J.D. Hanawalt, Powder Diffr. **1**, 7-13 (1986).
[36] K. Pye, S.J. Blott, Forensic Sci. Int. **144**, 19-27 (2004).
[37] S.J. Chung, A. Roy, D. Hong, J.P. Leonard, P.N. Kumta, Mater. Sci. Eng. B **176**, 1690-1694 (2011).
[38] L.A. Dobrzański, B. Tomiczek, G. Matula, K. Gołombek, Adv. Mat. Res. **939**, 84-89 (2014).
[39] M.K. Datta, Mater. Sci. Eng. B **176**, 1637-1643 (2011).